

# Time Harmonic interactions in the axisymmetric behaviour of transversely isotropic thermoelastic solid using New M-CST

Parveen Lata<sup>a</sup> and Harpreet Kaur\*

*Department of Basic and Applied Sciences, Punjabi University, Patiala, Punjab, India*

*(Received March 22, 2020, Revised July 11, 2020, Accepted October 19, 2020)*

**Abstract.** The present study is concerned with the thermoelastic interactions in a two dimensional homogeneous, transversely isotropic thermoelastic solid with new modified couple stress theory without energy dissipation and with two temperatures in frequency domain. The time harmonic sources and Hankel transform technique have been employed to find the general solution to the field equations. Concentrated normal force, normal force over the circular region, thermal point source and thermal source over the circular region have been taken to illustrate the application of the approach. The components of displacements, stress, couple stress and conductive temperature distribution are obtained in the transformed domain. The resulting quantities are obtained in the physical domain by using numerical inversion technique. Numerically simulated results are depicted graphically to show the effect of angular frequency on the resulted quantities.

**Keywords:** transversely isotropic; thermoelastic; time harmonic source; Hankel transform; new modified couple stress theory; two temperature

## 1. Introduction

Classical continuum theory with first gradient approach do not predict the size effects at nano and microscale. Therefore, a number of theories including higher gradients of deformation have been proposed to capture size-effects at the nano-scale. And, consideration of the second gradient of deformation leads naturally to the introduction of the idea of couple-stresses. Couple stress theory is such a higher order theory. This theory is an extension to continuum theory that includes the effects of couple stresses, in addition to the classical direct and shear forces per unit area. First mathematical model to examine the materials with couple stresses was presented by Cosserat and Cosserat (1909). This theory could not establish the constitutive relationships. Mindlin and Tierstein (1962) and Koiter (1964) developed initial version of couple stress theory, based on the Cosserat continuum theory (1909), involving length scale parameters to predict the size effects. It involves four material constants for isotropic elastic materials which are very difficult to determine experimentally (1964). So, Yang *et al.* (2002) presented modified couple stress theory (M-CST) with one length scale parameter, in which the couple stress tensor is symmetric. M-CST could not describe the pure bending of plate properly. So, Hadjesfandiari *et al.* (2011) gave consistent couple stress theory (C-

---

\*Corresponding author, Ph.D. Scholar, E-mail: mehrokpreet93@gmail.com

<sup>a</sup>Associate Professor, E-mail: parveenlata@pbi.ac.in

CST) with the skew-symmetric couple-stresses, that settles all the discrepancies of modified couple stress theory. Anisotropic materials are useful in engineering and medical. Modified couple stress theory was not applicable to anisotropic materials. So, Chen and Li (2014) presented the new modified couple stress theory (NM-CST) for anisotropic materials having three length scale parameters. Fakhrabadi (2017) studied the electromechanical behaviour of carbon nanotubes on the basis of modified couple stress theory and Homotopy perturbation method. Park and Gao (2006) studied the Bernoulli- Euler beam model based on a modified couple stress theory. Arani *et al.* (2015) studied the problem of vibration of bioliquid-filled microtubules embedded in cytoplasm including surface effects using the modified couple stress theory. Modified couple stress model has been developed for the dynamic study of Bernoulli-Euler beam by Kong *et al.* (2008) and for the solution of a simple shear problem by Park and Gao(2008) after deriving the boundary conditions and the governing differential equation of the theory in terms of the displacement. The static bending and free vibration problems of a Timoshenko beam are examined using modified couple stress theory by Ma *et al.* (2008). Tsiatas (2009) studied the static bending problem of Kirchhoff plates using modified couple stress theory. Tsiatas and Katsikadelis (2009) investigated the Saint-Venant's torsion problem of micro-bars using modified couple stress theory. Yin *et al.* (2010) investigated the vibration behaviour of Kirchhoff microplates in the context of modified couple stress theory and deriving the closed-form solution for natural frequency. Bending and vibration behaviours of Mindlin microplates were studied by Ma *et al.* (2011), in which the thickness stretching effect was also taken into account. Simsek *et al.* (2013) investigated the static bending of functionally graded microbeams based on the modified couple stress theory. Rafiq *et al.* (2019) studied the harmonic waves solution in dual phase lag magnatothermoelasticity. Kaushal *et al.* (2010) studied the response of frequency domain in generalized thermoelasticity with two temperatures. Chen *et al.* (2011) presented a new modified couple stress model for bending analysis of composite laminated beams with first order shear deformation. Problem of thermoelastic damping in the axisymmetric vibration of circular microplate resonators was examined by Fang *et al.* (2013) using two dimensional couple stress heat conduction model. Marin *et al.* (2017) studied the Saint-Venant's problem in the context of the theory of porous dipolar bodies. An axisymmetric problem of thick circular plate in modified couple stress theory of thermoelastic diffusion using Laplace and Hankel transforms technique is investigated by Kumar and Devi (2016). Atanasov *et al.* (2017) examined the thermal effect on the free vibration and buckling of the Euler-Bernoulli double microbeam system based on the modified couple stress theory using Bernoulli-Fourier method. Othman *et al.* (2013,2015) studied the thermo-microstretch elastic solid under the effect of gravity with energy dissipation using generalized theory of thermoelasticity. Sobhy and Radwan (2017) developed a nonlocal quasi-3D theory for the free vibration and buckling of FG nanoplates. Despite of this several researchers worked on the different theory of thermoelasticity as Marin (1998, 2009), Othman and Marin (2017), Arif *et al.* (2018), Lata (2018), Lata and Kaur (2019, 2019a, 2020, 2020a), El-Haina (2017), Ezzat *et al.* (2012, 2017), Kumar *et al.* (2016), Sharma *et al.* (2015), Othman and Abbas (2012), Fahsi *et al.* (2017), Abbas (2014, 2016), Karami *et al.* (2019, 2019a), Medani *et al.* (2019), Chaabane *et al.* (2019), Boulefrakh *et al.* (2019), Boukhelif *et al.* (2019), Boutaleb *et al.*(2019), Alimirzaei *et al.* (2019), Bourada *et al.* (2019), Zarga *et al.* (2019).

In the present study we deal with the thermoelastic interactions in a two dimensional homogeneous, transversely isotropic thermoelastic solids without energy dissipation and with two temperatures due to time harmonic sources in the context of new modified couple stress theory. The time harmonic sources and Hankel transforms have been employed to find the general solution to the field equations. Boundary plane is subjected to the normal and thermal sources. The components

of displacements, stresses and conductive temperature distribution are obtained in the transformed domain. Numerical computation is performed by using a numerical inversion technique and the resulting quantities are shown graphically to show the effect of angular frequency.

## 2. Basic equations

Following Chen and Li (2014), Sharma *et al.* (2015), the field equations for a transversely isotropic thermoelastic medium using new modified couple stress theory in the absence of body forces, body couple, mass diffusion sources and without energy dissipation are given by

$$\sigma_{ij} = c_{ijkl}\varepsilon_{kl} + \frac{1}{2}e_{ijk}m_{lk,l} - \beta_{ij}T, \quad (1)$$

$$c_{ijkl}\varepsilon_{kl,j} + \frac{1}{2}e_{ijk}m_{lk,lj} - \beta_{ij}T_{,j} = \rho\ddot{u}_i, \quad (2)$$

$$K_{ij}\varphi_{,ij} - \rho C_E \ddot{T} = \beta_{ij}T_0\ddot{\varepsilon}_{ij}, \quad (3)$$

where

$$\beta_{ij} = c_{ijkl}\alpha_{ij}, \quad (4)$$

$$\varepsilon_{ij} = \frac{1}{2}(u_{i,j} + u_{j,i}), \quad (5)$$

$$m_{ij} = l_i^2 G_i \chi_{ij} + l_j^2 G_j \chi_{ji}, \quad (6)$$

$$\chi_{ij} = \omega_{i,j}, \quad (7)$$

$$\omega_i = \frac{1}{2}e_{ijk}u_{k,j}, \quad (8)$$

and  $T = \varphi - a_{ij}\varphi_{,ij}$ ,  $K_{ij} = K_i\delta_{ij}$ .

Here,  $u = (u, v, w)$  is the components of displacement vector,  $c_{ijkl}$  ( $c_{ijkl} = c_{ijlk} = c_{jikl} = c_{jilk}$ ) are elastic parameters,  $a_{ij}$  are the two temperature parameters,  $\sigma_{ij}$  are the components of stress tensor,  $\varepsilon_{ij}$  are the components of strain tensor,  $e_{ijk}$  is alternate tensor,  $m_{ij}$  are the components of couple-stress,  $\alpha_{ij}$  are the coefficients of linear thermal expansion,  $\beta_{ij}$  is thermal tensor,  $T$  is the thermodynamical temperature,  $\varphi$  is the conductive temperature,  $l_i$  ( $i = 1, 2, 3$ ) are material length scale parameters,  $\chi_{ij}$  is curvature,  $\omega_i$  is the rotational vector,  $\rho$  is the density,  $K_{ij}$  is the materialistic constant,  $C_E$  is the specific heat at constant strain,  $T_0$  is the reference temperature assumed to be such that  $T/T_0 \ll 1$ ,  $G_i$  are the elasticity constants and  $\beta_1 = (c_{11} + c_{12})\alpha_1 + c_{13}\alpha_3$ ,  $\beta_3 = 2c_{13}\alpha_1 + c_{33}\alpha_3$ .

## 3. Formulation and solution of the problem

We consider a homogeneous transversely isotropic, thermoelastic body initially at uniform

temperature  $T_0$ . We take a cylindrical polar co-ordinate system  $(r, \theta, z)$  with symmetry about  $z$ -axis. As the problem considered is plane axisymmetric, the field component  $v = 0$ , and  $u, w, \varphi$  are independent of  $\theta$ . We have used appropriate transformation following Slaughter (2002) on the set of Eqs. (1)-(3) to derive the equations for transversely isotropic thermoelastic solid without energy dissipation and with two temperature and restrict our analysis to the two dimensional problem with  $\vec{u} = (u, 0, w)$ , we obtain

Equation of motion

$$c_{11} \left( \frac{\partial^2 u}{\partial r^2} + \frac{\partial u}{r \partial r} + \frac{u}{r} \right) + c_{44} \frac{\partial^2 u}{\partial z^2} + (c_{13} + c_{44}) \frac{\partial^2 w}{\partial r \partial z} - \frac{1}{4} l_2^2 G_2 \left( \frac{\partial^4 u}{\partial r^2 \partial z^2} - \frac{\partial^4 w}{\partial r^3 \partial z} + \frac{\partial^4 u}{\partial z^4} - \frac{\partial^4 w}{\partial r \partial z^3} \right) - \beta_1 \frac{\partial}{\partial r} \left( 1 - a_1 \left( \frac{\partial^2}{\partial r^2} + \frac{1}{r} \right) - a_3 \frac{\partial^2}{\partial z^2} \right) \varphi = \rho \ddot{u}, \quad (9)$$

$$c_{33} \frac{\partial^2 w}{\partial z^2} + (c_{44} + c_{13}) \left( \frac{\partial^2 u}{\partial r \partial z} + \frac{\partial u}{r \partial z} \right) + c_{44} \left( \frac{\partial^2 w}{\partial r^2} + \frac{\partial w}{r \partial r} \right) - \frac{1}{4} \left( -l_2^2 G_2 \left( -\frac{\partial^4 u}{\partial r^3 \partial z} + \frac{\partial^4 w}{\partial r^4} + \frac{1}{r} \left( -\frac{\partial^3 u}{\partial r^2 \partial z} + \frac{\partial^3 w}{\partial r^3} \right) \right) + l_2^2 G_2 \left( \frac{\partial^4 u}{\partial r^3 \partial z} - \frac{\partial^4 w}{\partial r^2 \partial z^2} + \frac{1}{r} \left( \frac{\partial^3 u}{\partial z^3} - \frac{\partial^3 w}{\partial r^2 \partial z} \right) \right) \right) - \beta_3 \frac{\partial}{\partial z} \left( 1 - a_1 \left( \frac{\partial^2}{\partial r^2} + \frac{1}{r} \right) - a_3 \frac{\partial^2}{\partial z^2} \right) \varphi = \rho \ddot{w}, \quad (10)$$

Equation of heat conduction without energy dissipation

$$K_1 \left( \frac{\partial^2 \varphi}{\partial r^2} + \frac{\varphi}{r} \right) + K_3 \frac{\partial^2 \varphi}{\partial z^2} - \rho c_E \frac{\partial^2}{\partial t^2} \left( 1 - a_1 \left( \frac{\partial^2}{\partial r^2} + \frac{1}{r} \right) - a_3 \frac{\partial^2}{\partial z^2} \right) \varphi = T_0 \frac{\partial^2}{\partial t^2} \left( \beta_1 \frac{\partial u}{\partial r} + \beta_3 \frac{\partial w}{\partial z} \right). \quad (11)$$

And the constitutive relationships are

$$\begin{aligned} \sigma_{zz} &= c_{13} e_{rr} + c_{13} e_{\theta\theta} + c_{33} e_{zz} - \beta_3 T, \\ \sigma_{rz} &= 2c_{44} e_{rz} - \frac{1}{4} \left( (l_1^2 G_1 - l_2^2 G_2) \left( -\frac{\partial^3 u}{\partial z \partial r^2} + \frac{\partial^3 w}{\partial r^3} \right) + (l_3^2 G_3 - l_2^2 G_2) \left( -\frac{\partial^3 u}{\partial z^3} + \frac{\partial^3 w}{\partial r \partial z^2} \right) \right), \\ \sigma_{\theta\theta} &= c_{21} e_{rr} + c_{11} e_{\theta\theta} + c_{13} e_{zz} - \beta_1 T, \\ \sigma_{rr} &= c_{11} e_{rr} + c_{12} e_{\theta\theta} + c_{13} e_{zz} - \beta_1 T, \\ m_{\theta z} &= \frac{1}{2} (l_2^2 G_2 - l_3^2 G_3) \left( \frac{\partial^2 u}{\partial z^2} - \frac{\partial^2 w}{\partial r \partial z} \right), \end{aligned} \quad (12)$$

where

$$e_{rr} = \frac{\partial u}{\partial r}, e_{\theta\theta} = \frac{u}{r}, e_{rz} = \frac{1}{2} \left( \frac{\partial u}{\partial z} + \frac{\partial w}{\partial r} \right), e_{zz} = \frac{\partial w}{\partial z}, T = \left( 1 - a_1 \left( \frac{\partial^2}{\partial r^2} + \frac{1}{r} \right) - a_3 \frac{\partial^2}{\partial z^2} \right) \varphi.$$

In the above equation we use contracting subscript notation ( $1 \rightarrow 11, 2 \rightarrow 22, 3 \rightarrow 33, 4 \rightarrow 23, 5 \rightarrow 31, 6 \rightarrow 12$ ) to relate  $c_{ijkl}$  to  $c_{mn}$ .

To facilitate the solution, the dimensionless quantities defined are defined as

$$\begin{aligned} \theta' &= \frac{\theta}{L}, r' = \frac{r}{L}, z' = \frac{z}{L}, t' = \frac{c_1}{L} t, u' = \frac{\rho c_1^2}{L \beta_1 T_0} u, w' = \frac{\rho c_1^2}{L \beta_1 T_0} w, T' = \frac{T}{T_0}, \sigma'_{zr} = \frac{\sigma_{zr}}{\beta_1 T_0}, \\ \sigma'_{rr} &= \frac{\sigma_{rr}}{\beta_1 T_0}, \sigma'_{z\theta} = \frac{\sigma_{z\theta}}{\beta_1 T_0}, m'_{z\theta} = \frac{m_{z\theta}}{L \beta_1 T_0}, a_1' = \frac{a_1}{L}, a_3' = \frac{a_3}{L}. \end{aligned} \quad (13)$$

Assuming the time harmonic behaviour as

$$(u, w, \varphi)(r, z, t) = (u, w, \varphi)(r, z) e^{i\omega t}, \quad (14)$$

where  $\omega$  is the angular frequency,

We define the Hankel transformation as

$$\tilde{f}(\xi, z, \omega) = \int_0^\infty f(r, z, \omega)rJ_n(r\xi)dr. \tag{15}$$

Using the dimensionless quantities defined by (13) on the set of Eqs. (9)-(11) and after suppressing the primes and then using (14)-(15) on the resulting equations yields

$$(-\epsilon_1 + \delta_2 D^2)\tilde{u} - \delta_1 \xi D \tilde{w} + \frac{1}{4L^2 c_{11}} l_2^2 G_2 ((\xi^2 D^2 - D^4)\tilde{u} - (\xi^3 D + \xi D^3)\tilde{w}) + \xi \left(1 + \frac{\alpha_1}{L} \xi^2 - \frac{\alpha_3}{L} D^2\right) \tilde{\varphi} = 0, \tag{16}$$

$$\delta_1 \epsilon_2 D \tilde{u} + (\epsilon_8 + \delta_3 D^2)\tilde{w} + \frac{\xi}{4L^2 c_{11}} \left(-l_2^2 G_2 (\xi^2 D \tilde{u} - \xi^3) + l_2^2 G_2 (D^3 \tilde{u} + D^2 \xi \tilde{w})\right) + \epsilon_9 D \left(1 + \frac{\alpha_1}{L} \xi^2 - \frac{\alpha_3}{L} D^2\right) \tilde{\varphi} = 0, \tag{17}$$

$$-\epsilon_6 \xi \omega^2 \tilde{u} - \epsilon_7 D \omega^2 \tilde{w} + \left(\epsilon_2 + \epsilon_5 D^2 + \epsilon_4 \omega^2 \left(1 + \frac{\alpha_1}{L} \xi^2 - \frac{\alpha_3}{L} D^2\right)\right) \tilde{\varphi} = 0, \tag{18}$$

where

$$\begin{aligned} \delta_1 &= \frac{c_{13} + c_{44}}{c_{11}}, & \delta_2 &= \frac{c_{44}}{c_{11}}, & \delta_3 &= \frac{c_{33}}{c_{11}}, & \epsilon_1 &= s^2 + \xi^2, & \epsilon_2 &= \frac{-\xi^2 + 1}{\xi}, & \epsilon_4 &= \frac{\rho c_E c_1^2}{K_1}, & \epsilon_5 &= \frac{K_3}{K_1}, \\ \epsilon_6 &= \frac{T_0 \beta_1^2}{K_1 \rho}, & \epsilon_7 &= \frac{T_0 \beta_1 \beta_3}{K_1 \rho}, & \epsilon_8 &= -\delta_2 \xi^2 - s^2, & \epsilon_9 &= \frac{\beta_3}{\beta_1}, & \epsilon_{10} &= \delta_2 + \frac{l_2^2 G_2}{4L^2 c_{11}} \xi^2, \\ \epsilon_{11} &= -\delta_1 \xi - \frac{l_2^2 G_2}{4L^2 c_{11}} \xi^3, & \epsilon_{12} &= \epsilon_8 + \frac{l_2^2 G_2}{4L^2 c_{11}} \xi^4, & \epsilon_{13} &= \epsilon_2 - \epsilon_4 s, & \epsilon_{14} &= \delta_3 + \xi^2 \frac{l_2^2 G_2}{4L^2 c_{11}}. \end{aligned}$$

The non-trivial solution of the system of the Eqs. (16)-(18) yields

$$(PD^8 + QD^6 + RD^4 + SD^2 + T) = 0, \tag{19}$$

Where

$$\begin{aligned} P &= -\epsilon_{26} \xi^2 \alpha_1^2, \\ Q &= \epsilon_{10} (\epsilon_{14} \epsilon_{26} - \epsilon_{16} \epsilon_{22}) + \alpha_1 (\epsilon_{12} \epsilon_{26} + \epsilon_{14} \epsilon_{25} - \epsilon_{16} \epsilon_{21}) - \xi \epsilon_{20} \alpha_1 \epsilon_{16} - \epsilon_{20} \epsilon_{14} \epsilon_{15} \\ &\quad + \xi \epsilon_{11} \alpha_1 \epsilon_{26} + \alpha_1 \xi (\epsilon_{27} \epsilon_{26} + \epsilon_2 \epsilon_{25} \alpha_1 - \epsilon_{22} \epsilon_{15}), \\ R &= -\epsilon_1 (\epsilon_{14} \epsilon_{26} - \epsilon_{16} \epsilon_{22}) + \epsilon_{10} (\epsilon_{12} \epsilon_{26} + \epsilon_{14} \epsilon_{25} - \epsilon_{16} \epsilon_{21}) + \alpha_1 (\epsilon_{12} - \epsilon_{25}) + \epsilon_{20} \epsilon_{27} \epsilon_{16} \\ &\quad + \xi \epsilon_{19} \alpha_1 \epsilon_{16} + \epsilon_{15} \epsilon_{19} \epsilon_{14} - \epsilon_{11} (\epsilon_{27} \epsilon_{26} - \xi \epsilon_{25} \alpha_1 - \epsilon_{22} \epsilon_{15}) + \alpha_1 \xi (\epsilon_{27} \epsilon_{25} + \epsilon_{15} \epsilon_{21}), \\ S &= -\epsilon_{11} (\epsilon_{27} \epsilon_{25} + \epsilon_{15} \epsilon_{21}) - \epsilon_{19} \epsilon_{27} \epsilon_{16} - \epsilon_{20} \epsilon_{15} \epsilon_{12} - \epsilon_1 (\epsilon_{12} \epsilon_{26} + \epsilon_{14} \epsilon_{25} - \epsilon_{16} \epsilon_{21}) \\ &\quad + \epsilon_{12} \epsilon_{10} \epsilon_{25}, \\ T &= -\epsilon_1 \epsilon_{12} \epsilon_{25} + \epsilon_{19} \epsilon_{12}. \end{aligned}$$

The roots of the Eq. (24) are  $\pm \lambda_i (i = 1, 2, 3, 4)$ , using the radiation condition that  $\hat{u}, \hat{w}, \hat{\varphi} \rightarrow 0$  as  $z \rightarrow \infty$ , the solution of Eq. (19) may be written as

$$(\tilde{u}, \tilde{w}, \tilde{\varphi}) = \sum_{i=1}^4 (1, R_i, S_i) A_i e^{-\lambda_i z}, \tag{20}$$

Where

$$R_i = \frac{-\epsilon_1 \epsilon_{25} + \epsilon_{15} \epsilon_{19} + (-\epsilon_1 \epsilon_{26} + \epsilon_{10} \epsilon_{25} + \epsilon_{15} \epsilon_{20}) \lambda_i^2 + (\epsilon_{10} \epsilon_{26} + \alpha_1 \epsilon_{13}) \lambda_i^4 + \alpha_1 \epsilon_{26} \lambda_i^6}{\epsilon_1 \epsilon_{25} + (\epsilon_{12} \epsilon_{26} + \epsilon_{14} \epsilon_{25} + \epsilon_{16} \epsilon_{21}) \lambda_i^2 + (\epsilon_{14} \epsilon_{26} - \epsilon_{16} \epsilon_{22}) \lambda_i^4}, \tag{21}$$

$$S_i = \frac{-\epsilon_1 \epsilon_{12} + (-\epsilon_1 \epsilon_{14} + \alpha_1 \epsilon_{12} - \epsilon_{27} \epsilon_{11}) \lambda_i^2 + (\epsilon_{10} \epsilon_{14} + \alpha_1 (\epsilon_{12} + \xi \epsilon_{27} + \xi \epsilon_{11})) \lambda_i^4 - \alpha_1 (-\epsilon_{14} + \xi^2 \alpha_1) \lambda_i^6}{\epsilon_1 \epsilon_{25} + (\epsilon_{12} \epsilon_{26} + \epsilon_{14} \epsilon_{25} + \epsilon_{16} \epsilon_{21}) \lambda_i^2 + (\epsilon_{14} \epsilon_{26} - \epsilon_{16} \epsilon_{22}) \lambda_i^4}, \tag{22}$$

and

$$\begin{aligned} \epsilon_{15} = -\epsilon_6\omega^2\xi, \epsilon_{16} = -\omega^2\epsilon_7, \epsilon_{17} = 1 + \frac{\alpha_1}{L}\xi^2, \epsilon_{18} = \frac{\alpha_3}{L}, \epsilon_{19} = -\xi\epsilon_{17}, \epsilon_{20} = \xi\epsilon_{18}, \epsilon_{21} = \\ \epsilon_9\epsilon_{17}, \epsilon_{22} = \epsilon_9\epsilon_{18}, \epsilon_{23} = -\omega^2\epsilon_4\epsilon_{17}, \epsilon_{24} = -\omega^2\epsilon_4\epsilon_{18}, \epsilon_{25} = -\epsilon_2 + \epsilon_{23}, \epsilon_{26} = -\epsilon_5 - \\ \epsilon_{24}, \epsilon_{27} = \epsilon_2\delta_1 + \alpha_1\xi^3, \alpha_1 = -\frac{l_2^2 G_2}{4L^2 c_{11}}. \end{aligned}$$

#### 4. Boundary conditions

For Mechanical forces/ Thermal sources acting on the surface  
The boundary conditions are

$$\sigma_{zz}(r, z, t) = -P_1(r, t), \quad (23)$$

$$\sigma_{zr}(r, z, t) = 0, \quad (24)$$

$$\frac{\partial \varphi}{\partial r}(r, z, t) = P_2(r, t)e^{i\omega t}, \quad (25)$$

$$m_{\theta z} = 0. \quad (26)$$

Here  $P_2(r, t) = 0$  corresponds to plane boundary subjected to normal force and  $P_1(r, t) = 0$  corresponds to plane boundary subjected to thermal point source.

##### 4.1 Applications

**Case I: Concentrated normal force/Thermal point source**-When plane boundary is subjected to concentrated normal force/ thermal point force, then  $P_1(r, t), P_2(r, t)$  take the form

$$(P_1(r, t), P_2(r, t)) = \left( \frac{P_1\delta(r)e^{i\omega t}}{2\pi r}, \frac{P_2\delta(r)e^{i\omega t}}{2\pi r} \right). \quad (27)$$

$P_1$  is the magnitude of the force applied,  $P_2$  is the magnitude of the constant temperature applied on the boundary and  $\delta(r)$  is the Dirac delta function. Applying Hankel transforms defined by (15) on Eq. (27), we get

$$\left( \widetilde{P}_1(\xi, \omega), \widetilde{P}_2(\xi, \omega) \right) = \left( \frac{P_1}{2\pi} e^{i\omega t}, \frac{P_2}{2\pi} e^{i\omega t} \right). \quad (28)$$

The expressions for the components of displacements, stress, couple stress and conductive temperature are given by the Eqs. (29)-(34).

$$\widetilde{u} = -\frac{P_1 e^{i\omega t}}{2\pi\Delta} \sum_{i=1}^4 B_{1i} e^{\lambda_i z} + \frac{P_2 e^{i\omega t}}{2\pi\Delta} \sum_{i=1}^4 B_{3i} e^{\lambda_i z}, \quad (29)$$

$$\widetilde{w} = -\frac{P_1 e^{i\omega t}}{2\pi\Delta} \sum_{i=1}^4 R_i B_{1i} e^{\lambda_i z} + \frac{P_2 e^{i\omega t}}{2\pi\Delta} \sum_{i=1}^4 R_i B_{3i} e^{\lambda_i z}, \quad (30)$$

$$\widetilde{\varphi} = -\frac{P_1 e^{i\omega t}}{2\pi\Delta} \sum_{i=1}^4 S_i B_{1i} e^{\lambda_i z} + \frac{P_2 e^{i\omega t}}{2\pi\Delta} \sum_{i=1}^4 S_i B_{3i} e^{\lambda_i z}, \quad (31)$$

$$\begin{aligned} \widetilde{\sigma}_{zz} = & -\frac{P_1 e^{i\omega t}}{2\pi\Delta} \sum_{i=1}^4 \left( \frac{\beta_1 T_0}{\rho c_1^2} (C_{13}\epsilon_2 - C_{33}\lambda_i R_i) - \beta_3 T_0 S_i \right) B_{1i} e^{\lambda_i z} \\ & + \frac{P_2 e^{i\omega t}}{2\pi\Delta} \sum_{i=1}^4 \left( \frac{\beta_1 T_0}{\rho c_1^2} (C_{13}\epsilon_2 - C_{33}\lambda_i R_i) - \beta_3 T_0 S_i \right) B_{3i} e^{\lambda_i z}, \end{aligned} \quad (32)$$

$$\begin{aligned} \widetilde{\sigma}_{zr} = & -\frac{P_1 e^{i\omega t}}{2\pi\Delta} \sum_{i=1}^4 \left( \frac{\beta_1 T_0}{\rho c_1^2} C_{44}(-\lambda_i - \xi R_i) - \beta_1 T_0 \left( \alpha_1(-\xi^2 \lambda_i - \xi^3 R_i) + \alpha_2(-\lambda_i^3 + \right. \right. \\ & \left. \left. \xi \lambda_i^2 R_i) \right) \right) B_{1i} e^{\lambda_i z} + \frac{P_2 e^{i\omega t}}{2\pi\Delta} \sum_{i=1}^4 \left( \frac{\beta_1 T_0}{\rho c_1^2} C_{44}(-\lambda_i - \xi R_i) - \beta_1 T_0 \left( \alpha_1(-\xi^2 \lambda_i - \xi^3 R_i) + \right. \right. \\ & \left. \left. \alpha_2(-\lambda_i^3 + \xi \lambda_i^2 R_i) \right) \right) B_{3i} e^{\lambda_i z} \end{aligned} \quad (33)$$

$$\begin{aligned} \widetilde{m}_{\theta z} = & -\frac{P_1 e^{i\omega t}}{2\Delta \rho c_1^2 L^2 (2\pi)} \sum_{i=1}^4 \beta_1 T_0 (l_1^2 G_1 - l_2^2 G_2) (\lambda_i^3 + \xi \lambda_i^2 R_i) B_{1i} e^{\lambda_i z} \\ & + \frac{P_2 e^{i\omega t}}{2\Delta \rho c_1^2 L^2 (2\pi)} \sum_{i=1}^4 \beta_1 T_0 (l_1^2 G_1 - l_2^2 G_2) (\lambda_i^3 + \xi \lambda_i^2 R_i) B_{3i} e^{\lambda_i z} \end{aligned} \quad (34)$$

**Case II: Normal force over the circular region/ Thermal source over the circular region**

Let a uniform pressure of total magnitude / constant temperature applied over a uniform circular region of radius  $a$  is obtained by setting

$$(P_1(r, t), P_2(r, t)) = \left( \frac{P_1}{\pi a^2} H(a - r) e^{i\omega t}, \frac{P_2}{\pi a^2} H(a - r) e^{i\omega t} \right). \quad (35)$$

where  $H(a - r)$  is the Heaviside unit step function.

Making use of dimensionless quantities defined by (13) & suppressing the primes, and then applying Harmonic behaviour and Hankel transforms defined by (14)-(15) on the resulting equation, we obtain

$$\left( \widetilde{P}_1(\xi, \omega), \widetilde{P}_2(\xi, \omega) \right) = \left( \frac{P_1}{\pi a \xi} J_1(a\xi) e^{i\omega t}, \frac{P_2}{\pi a \xi} J_2(a\xi) e^{i\omega t} \right). \quad (36)$$

The expressions for the components of displacements, stress, couple stress and conductive temperature are obtained by replacing  $\frac{P_1}{2\pi}$  with  $\frac{P_1 J_1(a\xi)}{\pi a \xi}$  and by replacing  $\frac{P_2}{2\pi}$  with  $\frac{P_2 J_1(a\xi)}{\pi a \xi}$  in Eqs. (30)-(34) and are given by (37)-(42).

**For circular region**

$$\widetilde{u} = -\frac{P_1 e^{i\omega t}}{\Delta} \sum_{i=1}^4 \frac{J_1(a\xi)}{\pi a \xi} B_{1i} e^{\lambda_i z} + \frac{P_2 e^{i\omega t}}{\Delta} \sum_{i=1}^4 \frac{J_1(a\xi)}{\pi a \xi} B_{3i} e^{\lambda_i z}, \quad (37)$$

$$\widetilde{w} = -\frac{P_1 e^{i\omega t}}{\Delta} \sum_{i=1}^4 R_i \frac{J_1(a\xi)}{\pi a \xi} B_{1i} e^{\lambda_i z} + \frac{P_2 e^{i\omega t}}{\Delta} \sum_{i=1}^4 R_i \frac{J_1(a\xi)}{\pi a \xi} B_{3i} e^{\lambda_i z} \quad (38)$$

$$\widetilde{\phi} = -\frac{P_1 e^{i\omega t}}{\Delta} \sum_{i=1}^4 R_i \frac{J_1(a\xi)}{\pi a \xi} B_{1i} e^{\lambda_i z} + \frac{P_2 e^{i\omega t}}{\Delta} \sum_{i=1}^4 R_i \frac{J_1(a\xi)}{\pi a \xi} B_{3i} e^{\lambda_i z} \quad (39)$$

$$\begin{aligned} \widetilde{\sigma}_{zz} = & -\frac{P_1 e^{i\omega t}}{\Delta} \sum_{i=1}^4 \left( \frac{\beta_1 T_0}{\rho c_1^2} (C_{13} \epsilon_2 - C_{33} \lambda_i R_i) - \beta_3 T_0 S_i \right) \sum_{i=1}^4 \frac{J_1(a\xi)}{\pi a \xi} B_{1i} e^{\lambda_i z} + \\ & \frac{P_2 e^{i\omega t}}{\Delta} \sum_{i=1}^4 \left( \frac{\beta_1 T_0}{\rho c_1^2} (C_{13} \epsilon_2 - C_{33} \lambda_i R_i) - \beta_3 T_0 S_i \right) \sum_{i=1}^4 \frac{J_1(a\xi)}{\pi a \xi} B_{3i} e^{\lambda_i z}, \end{aligned} \quad (40)$$

$$\widetilde{\sigma}_{zr} = -\frac{P_1 e^{i\omega t}}{\Delta} \sum_{i=1}^4 \left( \frac{\beta_1 T_0}{\rho c_1^2} C_{44}(-\lambda_i - \xi R_i) - \beta_1 T_0 \left( \alpha_1(-\xi^2 \lambda_i - \xi^3 R_i) + \alpha_2(-\lambda_i^3 + \right. \right. \quad (41)$$

$$\xi \lambda_i^2 R_i)) \left) \frac{J_1(a\xi)}{\pi a \xi} B_{1i} e^{\lambda_i z} + \frac{P_2 e^{i\omega t}}{\Delta} \sum_{i=1}^4 \left( \frac{\beta_1 T_0}{\rho c_1^2} C_{44} (-\lambda_i - \xi R_i) - \beta_1 T_0 (\alpha_1 (-\xi^2 \lambda_i - \xi^3 R_i) + \alpha_2 (-\lambda_i^3 + \xi \lambda_i^2 R_i)) \right) \frac{J_1(a\xi)}{\pi a \xi} B_{3i} e^{\lambda_i z},$$

$$\widetilde{m}_{\theta z} = -\frac{P_1 e^{i\omega t}}{2\Delta \rho c_1^2 L^2} \sum_{i=1}^4 \beta_1 T_0 (l_1^2 G_1 - l_2^2 G_2) (\lambda_i^3 + \xi \lambda_i^2 R_i) \frac{J_1(a\xi)}{\pi a \xi} B_{1i} e^{\lambda_i z} + \frac{P_2 e^{i\omega t}}{2\Delta \rho c_1^2 L^2} \sum_{i=1}^4 \beta_1 T_0 (l_1^2 G_1 - l_2^2 G_2) (\lambda_i^3 + \xi \lambda_i^2 R_i) \frac{J_1(a\xi)}{\pi a \xi} B_{3i} e^{\lambda_i z}. \tag{42}$$

where

$$A_{1i} = \frac{\beta_1 T_0}{\rho c_1^2} (C_{13} \epsilon_2 - C_{33} \lambda_i R_i) - \beta_3 T_0 S_i,$$

$$A_{2i} = \frac{\beta_1 T_0}{\rho c_1^2} C_{44} (-\lambda_i - \xi R_i) - \beta_1 T_0 (\alpha_1 (-\xi^2 \lambda_i - \xi^3 R_i) + \alpha_2 (-\lambda_i^3 + \xi \lambda_i^2 R_i)),$$

$$A_{3i} = -\lambda_i S_i,$$

$$A_{4i} = \frac{\beta_1 T_0}{2\rho c_1^2 L^2} (l_1^2 G_1 - l_2^2 G_2) (\lambda_i^2 - \xi \lambda_i R_i), \quad i = 1, 2, 3, 4 .$$

$$\Delta = \Delta_1 - \Delta_2 + \Delta_3 - \Delta_4,$$

$$\Delta_1 = A_{11} A_{22} (A_{33} A_{44} - A_{43} A_{34}) - A_{11} A_{23} (A_{32} A_{44} - A_{42} A_{34}) + A_{11} A_{24} (A_{32} A_{43} - A_{42} A_{33}),$$

$$\Delta_2 = A_{12} A_{21} (A_{33} A_{44} - A_{43} A_{34}) - A_{12} A_{23} (A_{31} A_{44} - A_{41} A_{34}) + A_{24} A_{12} (A_{31} A_{43} - A_{41} A_{33}),$$

$$\Delta_3 = A_{13} A_{21} (A_{32} A_{44} - A_{42} A_{34}) - A_{22} A_{13} (A_{31} A_{44} - A_{41} A_{34}) + A_{13} A_{24} (A_{31} A_{42} - A_{41} A_{32}),$$

$$\Delta_4 = A_{14} A_{21} (A_{32} A_{43} - A_{42} A_{33}) - A_{22} A_{14} (A_{31} A_{43} - A_{41} A_{33}) + A_{14} A_{23} (A_{31} A_{42} - A_{41} A_{32}),$$

$$B_{11} = \Delta_1 / A_{11},$$

$$B_{12} = -\Delta_2 / A_{12},$$

$$B_{13} = \Delta_3 / A_{13},$$

$$B_{14} = -\Delta_4 / A_{14},$$

$$A_i = \frac{1}{\Delta} (\widetilde{P}_1(\xi, \omega) B_{1i} + \widetilde{P}_2(\xi, \omega) B_{3i}),$$

$$B_{31} = A_{12} (A_{23} A_{44} - A_{43} A_{24}) - A_{13} (A_{22} A_{44} - A_{42} A_{24}) + A_{14} (A_{22} A_{43} - A_{42} A_{23}),$$

$$B_{32} = -A_{11} (A_{23} A_{44} - A_{43} A_{24}) + A_{13} (A_{21} A_{44} - A_{41} A_{24}) - A_{14} (A_{21} A_{43} - A_{41} A_{23}),$$

$$B_{33} = A_{11} (A_{22} A_{44} - A_{42} A_{24}) - A_{12} (A_{21} A_{44} - A_{41} A_{24}) + A_{14} (A_{21} A_{42} - A_{41} A_{22}),$$

$$B_{34} = -A_{11} (A_{22} A_{43} - A_{42} A_{23}) + A_{12} (A_{21} A_{43} - A_{41} A_{23}) - A_{13} (A_{21} A_{42} - A_{41} A_{22}).$$

### 6. Inversion of the transformations

To obtain the solution of the problem in physical domain, we must invert the transforms in Eqs. (31)-(36) and (37)-(42). Here the displacement components, normal and tangential stresses ,conductive temperature and couple stress are functions of z, the parameter of Hankel transform is  $\xi$  and hence are of the form  $\tilde{f}(\xi, z)$ . To obtain the function  $f(r, z)$  in the physical domain, we first invert the Hankel transform using

$$f(r, z) = \int_0^\infty \xi \tilde{f}(\xi, z) J_n(\xi r) d\xi. \tag{43}$$

The last step is to calculate the integral in Eq. (43). The method for evaluating this integral is described in Press *et al.* (1986). It involves the use of Romberg’s integration with adaptive step size. This also uses the results from successive refinements of the extended trapezoidal rule followed by

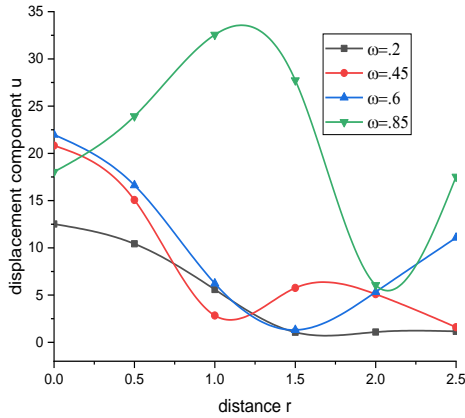


Fig. 1 variation of displacement  $u$  with the distance  $r$  (concentrated normal force)

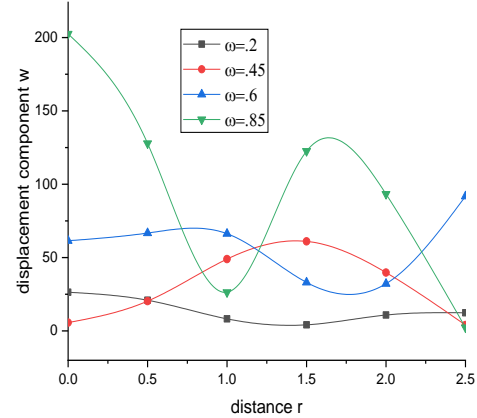


Fig. 2 variation of displacement  $w$  with the distance  $r$  (concentrated normal force)

extrapolation of the results to the limit when the step size tends to zero.

## 7. Results and discussions

For numerical computations, we take the copper material which is transversely isotropic

$$\begin{aligned} c_{11} &= 18.78 \times 10^{10} \text{ Kgm}^{-1}\text{s}^{-2}, & c_{12} &= 8.76 \times 10^{10} \text{ Kgm}^{-1}\text{s}^{-2}, & c_{13} &= 8.0 \times 10^{10} \text{ Kgm}^{-1}\text{s}^{-2}, \\ c_{33} &= 17.2 \times 10^{10} \text{ Kgm}^{-1}\text{s}^{-2}, & c_{44} &= 5.06 \times 10^{10} \text{ Kgm}^{-1}\text{s}^{-2}, & C_E &= 0.6331 \times 10^3 \text{ JKg}^{-1}\text{K}^{-1}, \end{aligned}$$

$$\begin{aligned} \alpha_1 &= 2.98 \times 10^{-5} \text{ K}^{-1}, & \alpha_3 &= 2.4 \times 10^{-5} \text{ K}^{-1}, & T_0 &= 293 \text{ K}, & \rho &= 8.954 \times 10^3 \text{ Kgm}^{-3}, \\ K_1 &= 0.433 \times 10^3 \text{ Wm}^{-1}\text{K}^{-1}, & K_3 &= 0.450 \times 10^3 \text{ Wm}^{-1}\text{K}^{-1}, & G_1 &= 0.1, & G_2 &= 0.2, \\ G_3 &= 0.3, & L &= 1, & l_1 &= l_2 = l_3 = .243 \text{ nm}, & a_1 &= .01, & a_3 &= .02. \end{aligned}$$

The values of displacements  $u$  and  $w$ , normal force stress  $\sigma_{zz}$ , tangential stress  $\sigma_{zr}$  and conductive temperature  $\varphi$  for a transversely isotropic thermoelastic solid with two temperature are determined with the help of software GNU Octave 5.1.0 and presented graphically with the help of OriginPro 2018 to show the impact of harmonic behaviour varying the angular frequency for the four different values i)  $\omega = .2$  ii)  $\omega = .45$  iii)  $\omega = .6$ . (iv)  $\omega = .85$ . Analysis has been done by varying the distance  $r$  from 0 to 2.5.

- i) The solid line in black with centre symbol square corresponds to  $\omega = .2$ .
- ii) The solid line in red with centre symbol circle corresponds to  $\omega = .45$ .
- iii) The solid line in blue with centre symbol triangle corresponds to  $\omega = .6$ .
- iv) The solid line in green with centre symbol inverted triangle corresponds to  $\omega = .85$ .

### 7.1 Normal force on the boundary of the half-space

#### Case 1: Concentrated normal force

Figs. 1-6 depicts the characteristics of concentrated normal force. In Fig. 1 curves depicting the variation of displacement  $u$ , corresponding to the frequencies  $\omega = .2, \omega = .45$  and  $\omega = .6$

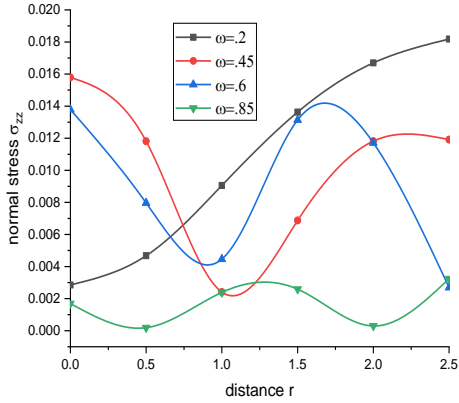


Fig. 3 variation of conductive temperature  $\varphi$  with the distance  $r$  (concentrated normal force)

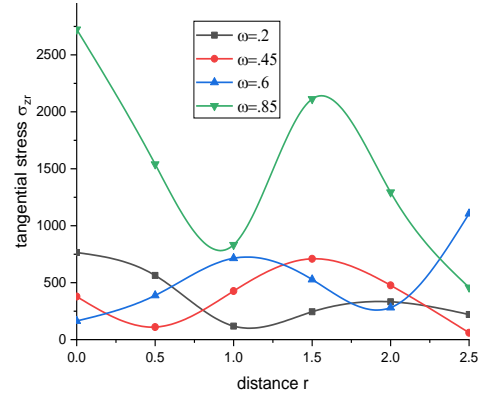


Fig. 4 variation of tangential stress  $\sigma_{zr}$  with the distance  $r$  (concentrated normal force)

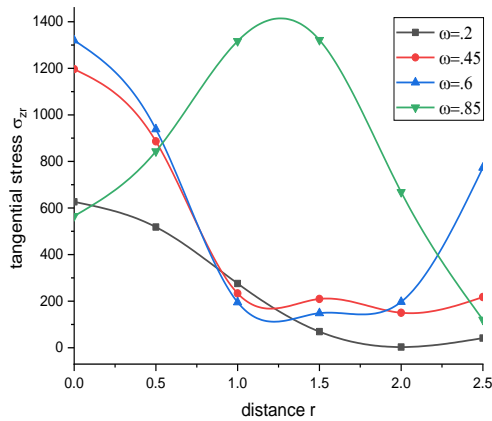


Fig. 5 variation of normal stress  $\sigma_{zz}$  with the distance  $r$  (concentrated normal force)

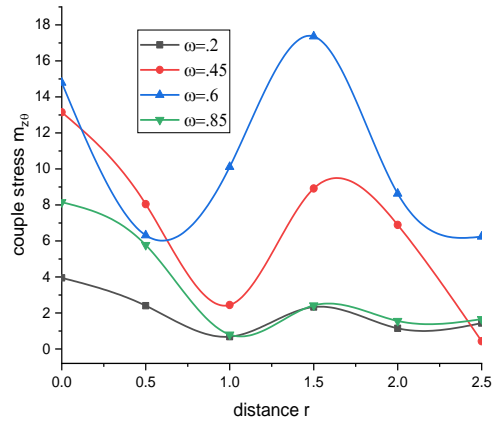


Fig. 6 variation of couple stress  $m_{z\theta}$  with the distance  $r$  (concentrated normal force)

monotonically and rapidly decrease in the range  $0 \leq r \leq 1.5$  and increase in the rest of the range slightly.  $\omega = .85$  leads to the asymmetry in the variation of the characteristic curves. Here we observe that increase in frequency increases the magnitude of variations. Characteristic curve for  $\omega = .85$  monotonically increase in  $0 \leq r \leq 1$  and  $2 \leq r \leq 2.5$  and monotonically decreases in the rest of the range. In Fig. 2 curves depicting the variation of displacement  $w$  do not follow a symmetric pattern. Displacement  $w$  corresponding to the frequencies  $\omega = .2$  and  $\omega = .6$  decreases in the  $0 \leq r \leq 1.5$  and increases in the remaining range of distance  $r$  with the difference in magnitude of the each curve. Value of the displacement  $w$  for the frequency  $\omega = .45$  increases in the first half of the distance axes and decreases in the remaining range. Characteristic curve for  $\omega = .85$  monotonically decrease in  $0 \leq r \leq 1$  and  $2 \leq r \leq 2.5$  and monotonically increases in the rest of the range. Amplitude is largest in case of  $\omega = .85$ . In Fig. 3 curves for the variation of Conductive temperature  $\varphi$  corresponding to the frequency  $\omega = .2$  increase from .004 to .018 with the increase of  $r$ , and corresponding to the frequencies  $\omega = .45$  and  $\omega = .6$  decreases in  $0 \leq r \leq 1$  and  $2 \leq r \leq 2.5$  and increases in the rest of the range. Value of  $\varphi$  corresponding to the  $\omega = .85$

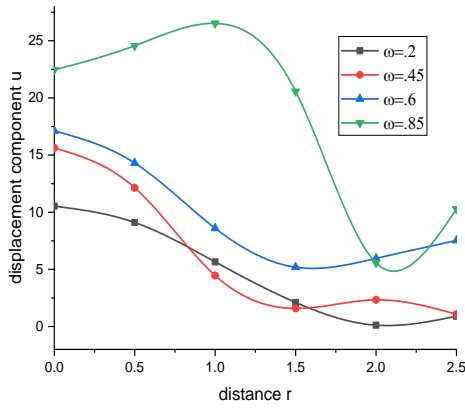


Fig. 7 Variation of displacement  $u$  with the distance  $r$  (normal force over the circular region)

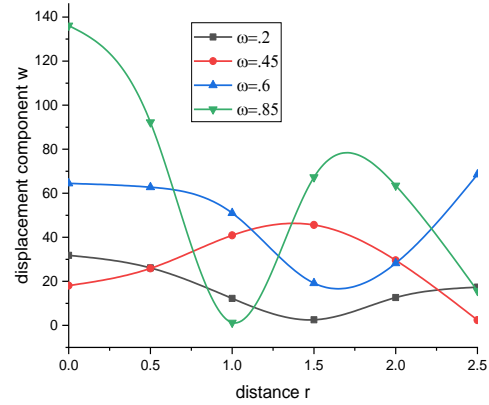


Fig. 8 Variation of displacement  $w$  with the distance  $r$  (normal force over the circular region)

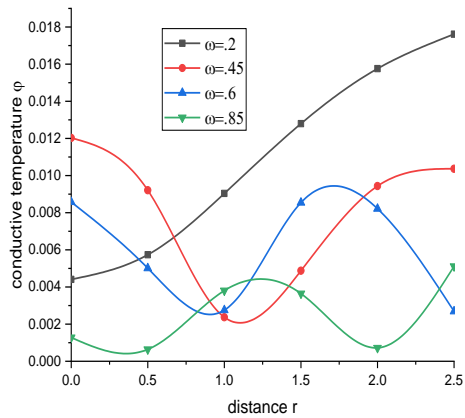


Fig. 9 Variation of conductive temperature  $\phi$  with the distance  $r$  (normal force over the circular region)

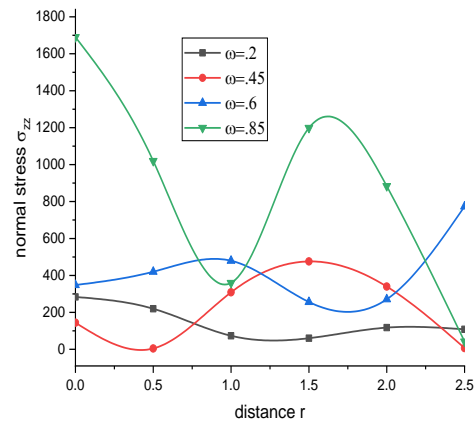


Fig. 10 Variation of normal stress  $\sigma_{zz}$  with the distance  $r$  (normal force over the circular region)

shows oscillatory behavior with the distance  $r$ . In Fig. 4 variation of the normal stress  $\sigma_{zz}$  is similar to the displacement  $w$ , except for the  $\omega = .45$ . Curve corresponding to the  $\omega = .45$  decreases in  $0 \leq r \leq 0.5$  and  $1.5 \leq r \leq 2.5$  and increases only in the range  $0.5 \leq r \leq 1.5$ . In Fig. 5 tangential stress  $\sigma_{zr}$  decreases for  $0 \leq r \leq 1.5$  and increases for the rest corresponding to the  $\omega = .45$  and the  $\omega = .6$ .  $\sigma_{zr}$  decreases monotonically with the increases in  $r$ . Corresponding to the  $\omega = .85$ , value of  $\sigma_{zr}$  monotonically increases for  $0 \leq r \leq 1.5$  and decreases in the rest. In Fig. 6 couple stress  $m_{z\theta}$  corresponding to the frequencies  $\omega = .45$  and  $\omega = .6$  decreases smoothly for  $0 \leq r \leq 1$  and  $2 \leq r \leq 2.5$  and increase in the rest.  $m_{z\theta}$  for  $\omega = .2$  follow oscillatory trend, with the small amplitude of the variation. Corresponding to the  $\omega = .85$  couple stress decreases in the  $0 \leq r \leq 1$  and maintains constant value in the remaining range.

**Case 2: Normal force over the circular region**

Figs. 7-12 show the characteristics of concentrated normal force. In Figs. 7-10 characteristic curves for the variation of displacements, conductive temperature  $\phi$  and normal stress  $\sigma_{zz}$  resp. are

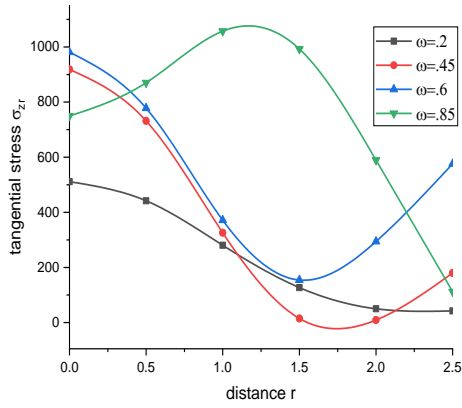


Fig. 11 Variation of tangential stress  $\sigma_{zr}$  with the distance  $r$  (normal force over the circular region)

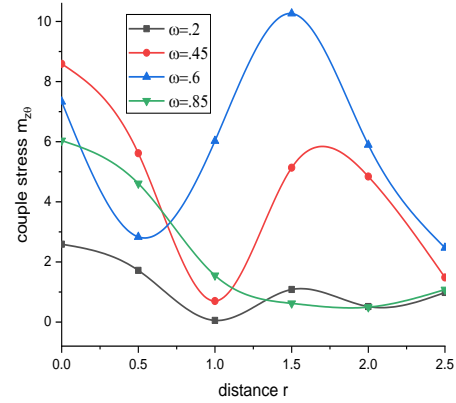


Fig. 12 Variation of couple stress  $m_{z\theta}$  with the distance  $r$  (normal force over the circular region)

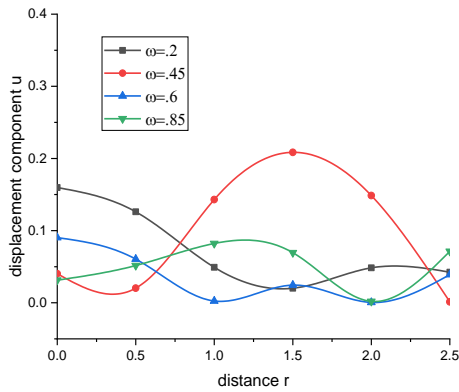


Fig. 13 variation of displacement  $u$  with the distance  $r$  (thermal point source)

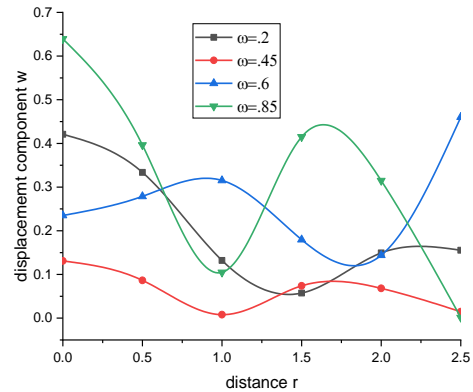


Fig. 14 variation of displacement  $w$  with the distance  $r$  (thermal point source)

similar to the corresponding characteristics curve of the normal force over the circular region, expect for the amplitude of the curve. In Fig. 11 tangential stress  $\sigma_{zr}$  corresponding to the  $\omega = .2$  and  $\omega = .45$  follow descending oscillatory behavior with the distance  $r$ . Corresponding to the frequency  $\omega = .6$ , decreases for the range  $0 \leq r \leq 1$ , almost constant magnitude for the  $1 \leq r \leq 2$  and increases in the rest. Value of  $\sigma_{zr}$  decreases in the range  $0 \leq r \leq 2.2$  and increases in very small range of the distance axes. At the origin, as the angular frequency increases value of the tangential stress reduces. In Fig. 12, curves showing the variation of couple stress  $m_{z\theta}$  follow oscillatory behaviour with intermediate amplitude. Curve corresponding to  $\omega = .25$  is descending oscillatory.

### 7.2 Thermal source on the boundary of half-space

#### Case-I: Thermal point source

The Figs. 13-18 correspond to the characteristics of thermal point source. In Fig. 13 curves for the variation of displacement  $u$  corresponding to  $\omega = .2$  and  $\omega = .6$  monotonically decrease for  $0 \leq r \leq 1.5$  and increase in the remaining range. curves corresponding to  $\omega = .85$  monotonically

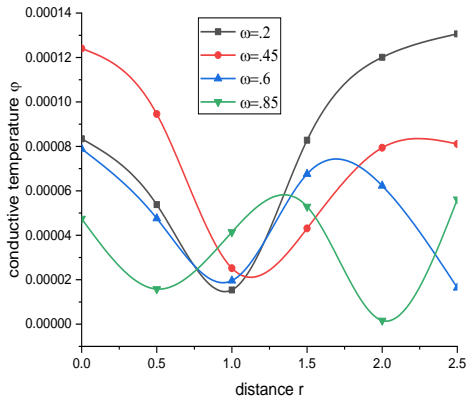


Fig. 15 Variation of conductive temperature  $\varphi$  with the distance  $r$  (thermal point source)

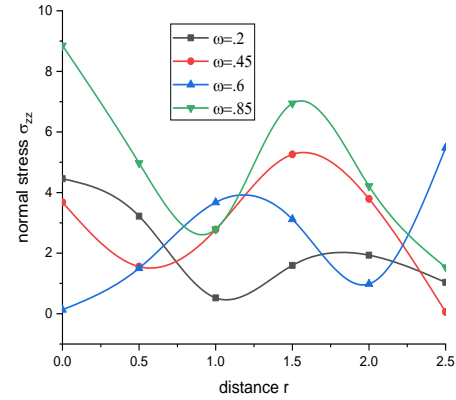


Fig. 16 Variation of normal stress  $\sigma_{zz}$  with the distance  $r$  (thermal point source)

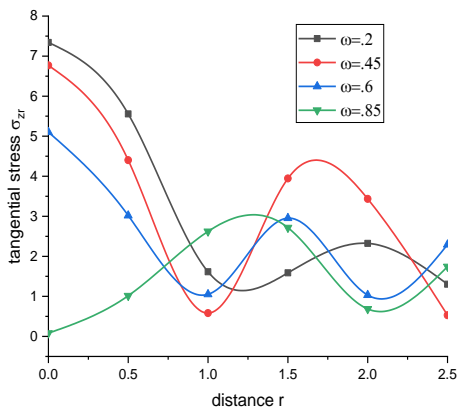


Fig. 17. Variation of normal stress  $\sigma_{zz}$  with the distance  $r$  (thermal point source)

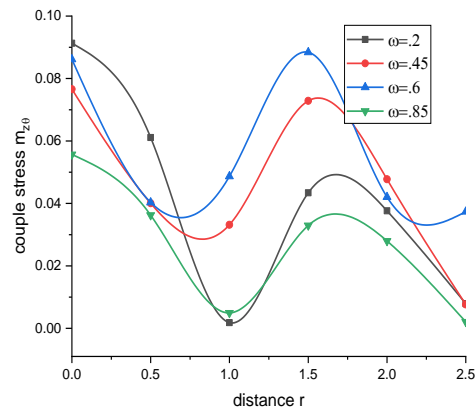


Fig. 18 Variation of couple stress  $m_{z\theta}$  with the distance  $r$  (thermal point source)

increase for the  $0 \leq r \leq 1.5$  and  $2 \leq r \leq 2.5$ , and decrease in the rest of the range. Value of displacement  $u$  corresponding to  $\omega = .45$  is almost constant for  $0 \leq r \leq 0.5$ , monotonically increase in the range  $0.5 \leq r \leq 1.5$  and decreases in the remaining range. Amplitude of the variation is large in the range  $1 \leq r \leq 2$  for  $\omega = .45$ . In Fig. 14, displacement  $w$  corresponding to the frequencies  $\omega = .2, \omega = .45$  and  $\omega = .85$  monotonically decrease in the range  $0 \leq r \leq 1$  and increase in  $1 \leq r \leq 1.7$  and again decrease in the remaining range, but with difference in the amplitude of the variation corresponding to each frequency. Curve corresponding to the frequency  $\omega = .6$  shows inverse behaviour to the remaining cases. In Fig. 15, conductive temperature  $\varphi$  decrease for  $0 \leq r \leq 1$  and increase for the  $1 \leq r \leq 1.5$  and decrease in the remaining range corresponding to all the frequencies  $\omega = .2, \omega = .45, \omega = .6$  and  $\omega = .85$ . In Fig. 16, normal stress  $\sigma_{zz}$  decreases for  $0 \leq r \leq 1$  and increases for the  $1 \leq r \leq 1.5$  and again decreases in the remaining range corresponding to  $\omega = .2, \omega = .45$  and  $\omega = .85$ . Curve corresponding to the  $\omega = .6$  shows inverse behaviour to all the remaining three cases. In Fig. 17, tangential stress  $\sigma_{zr}$  decreases for  $0 \leq r \leq 1$  and increases for the  $1 \leq r \leq 1.5$  and again decreases

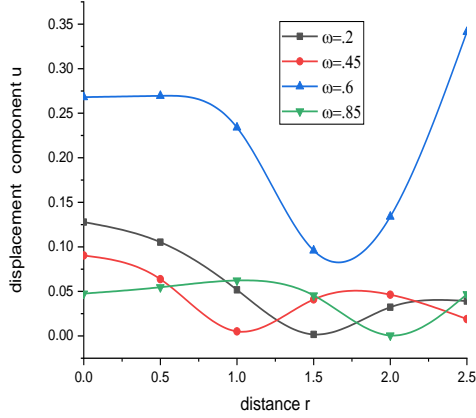


Fig. 19 Variation of displacement  $u$  with the distance  $r$  (thermal source over the circular region)

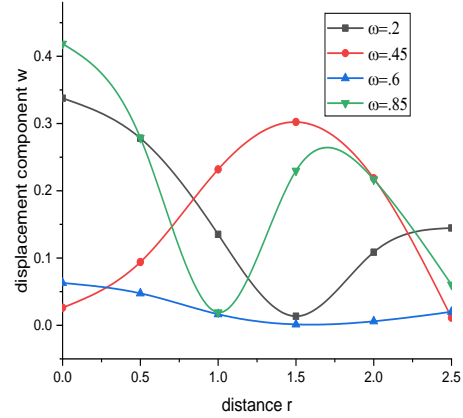


Fig. 20 Variation of displacement  $w$  with the distance  $r$  (thermal source over the circular region)

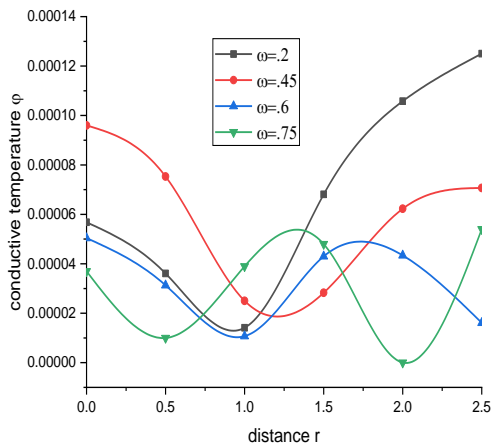


Fig. 21 Variation of conductive temperature  $\phi$  with the distance  $r$  (thermal source over the circular region)

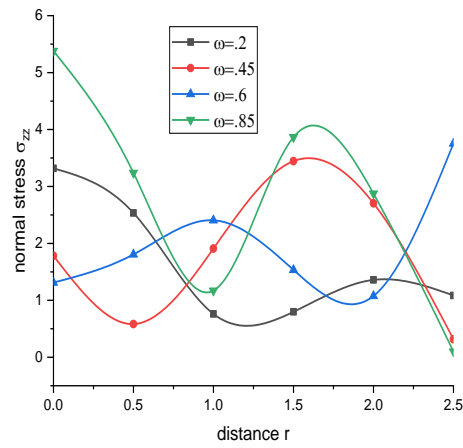


Fig. 22 variation of tangential stress  $\sigma_{zr}$  with the distance  $r$  (thermal source over the circular region)

in the remaining range corresponding to  $\omega = .2$ ,  $\omega = .45$  and  $\omega = .6$ . Curve corresponding to the  $\omega = .85$  shows inverse increasing and decreasing behaviour to all the remaining three cases. In Fig. 18 the couple stress  $m_{z\theta}$  corresponding to all the four frequencies decreases monotonically for  $0 \leq r \leq 1$  and increases for the  $1 \leq r \leq 1.8$  and again, decreases in the remaining range.

**Case-II: Thermal source over the circular region**

Figs. 19-24 depict the characteristics of the thermal source over the circular region. In Fig. 19 displacement  $u$  show oscillatory behaviour corresponding to the frequencies  $\omega = .2$ ,  $\omega = .45$  and  $\omega = .85$ . Amplitude of the variation is small in the three cases. Curve corresponding to  $\omega = .6$  shows constant variation for  $0 \leq r \leq 1$  and decreases for the  $1 \leq r \leq 1.7$  and increases in the remaining range. In Fig. 20 displacement  $w$  corresponding to  $\omega = .2$  and  $\omega = .6$  decreases for  $0 \leq r \leq 1.5$  and increases in the rest. Amplitude of the variation is very small in the latter case. Curve corresponding to  $\omega = .45$  shows inverse behaviour to  $\omega = .2$ . Variation of the displacement  $w$

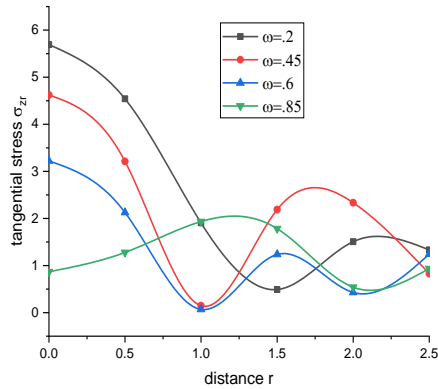


Fig. 23 Variation of normal stress  $\sigma_{zz}$  with the distance  $r$  (thermal source over the circular region)

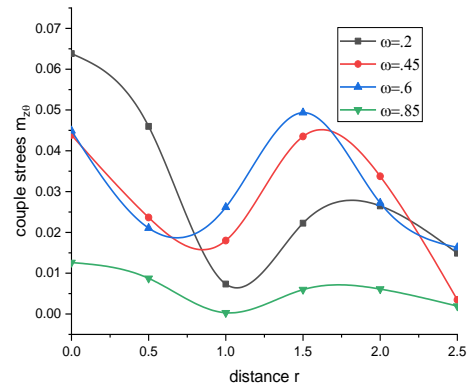


Fig. 24 Variation of couple stress  $m_{z\theta}$  with the distance  $r$  (thermal source over the circular region)

corresponding to  $\omega = .85$  monotonically decreases in the range  $0 \leq r \leq 1$  and  $2 \leq r \leq 2.5$  and increases in the remaining range. In Fig. 30, Characteristic curves for the variation of conductive temperature  $\varphi$ , normal stress  $\sigma_{zz}$ , tangential stress  $\sigma_{zr}$  and the couple stress  $m_{z\theta}$  are similar to the corresponding characteristics curves of the thermal point source, expect for the amplitude and magnitude of the variation.

## 7. Conclusions

This investigation dealt with the study of transversely isotropic thermoelastic medium in the context of new modified couple stress theory with two temperature. The mathematical expressions for displacements, conductive temperature, stress and couple stress have been derived in frequency domain. From the above discussion it is clear that the effect of frequency plays an important role in the study of the deformation of the transversely isotropic thermoelastic body in the context of new modified couple stress theory. As  $r$  varies from the loading surface/boundary surface, the components of displacements, normal stress, tangential stress, couple stress and conductive temperature for normal forces and thermal sources follow different types of pattern. It is observed that the variation of resulting quantities obtained after the numerical computation is oscillatory almost in all the cases with difference in magnitude/value. Appreciable effect of frequency is observed on the resulted quantities. The results of this problem are very useful for the people who are working in the various fields of geophysics, electronics and seismology.

## References

- Abbas, I.A. (2014), "Three-phase lag model on thermoelastic interaction in an unbounded fiber-reinforced anisotropic medium with a cylindrical cavity", *J. Comput. Theo. Nanosci.*, **11**(4), 987-992. <https://doi.org/10.1166/jctn.2014.3454>.
- Abbas, I.A. (2016), "Free vibration of a thermoelastic hollow cylinder under two-temperature generalized thermoelastic theory", *Mech. Bas. Des. Struct. Mach.*, **45**(3), 395-405. <https://doi.org/10.1080/15397734.2016.1231065>.

- Alimirzaei, S., Mohammadimehr, M. and Tounsi, A. (2019), "Nonlinear analysis of viscoelastic micro-composite beam with geometrical imperfection using FEM: MSGT electro-magneto-elastic bending, buckling and vibration solutions", *Struct. Eng. Mech.*, **71**(5), 485-502. <https://doi.org/10.12989/sem.2019.71.5.485>.
- Arani Ghorbanpour, A., Abdollahian, M. and Jalaei, H.M. (2015), "Vibration of bioliquid-filled microtubules embedded in cytoplasm including surface effects using modified couple stress theory", *J. Theo. Biology*, **367**, 29-38. <https://doi.org/10.1016/j.jtbi.2014.11.019>.
- Arif, S.M., Biwi, M. and Jahangir, A. (2018), "Solution of algebraic lyapunov equation on positive-definite hermitian matrices by using extended Hamiltonian algorithm", *Comput. Mater. Continua*, **54**, 181-195.
- Atanasov, M.S., Karličić, D., Kozić, P. and Janevski, G. (2017), "Thermal effect on free vibration and buckling of a double-microbeam system", *Facta Universitatis, Series: Mech. Eng.*, **15**(1), 45-62. <https://doi.org/10.22190/FUME161115007S>.
- Boukhelif, Z., Bouremana, M., Bourada, F., Bousahla, A.A., Bourada, M., Tounsi, A. and Al-Osta, M.A. (2019), "A simple quasi-3D HSDT for the dynamics analysis of FG thick plate on elastic foundation", *Steel Compos. Struct.*, **31**(5), 503-516. <https://doi.org/10.12989/scs.2019.31.5.503>.
- Boulefrakh, L., Hebali, H., Chikh, A., Bousahla, A.A., Tounsi, A. and Mahmoud, S.R. (2019), "The effect of parameters of visco-Pasternak foundation on the bending and vibration properties of a thick FG plate", *Geomech. Eng.*, **18**(2), 161-178. <https://doi.org/10.12989/gae.2019.18.2.161>.
- Bourada, F., Bousahla, A.A., Bourada, M., Azzaz, A., Zinata, A. and Tounsi, A. (2019), "Dynamic investigation of porous functionally graded beam using a sinusoidal shear deformation theory", *Wind Struct.*, **28**(1), 19-30. <https://doi.org/10.12989/was.2019.28.1.019>.
- Boutaleb, S., Benrahou, K.H., Bakora, A., Algarni, A., Bousahla, A.A., Tounsi, A., Mahmoud, S.R. and Tounsi, A. (2019), "Dynamic analysis of nanosize FG rectangular plates based on simple nonlocal quasi 3D HSDT", *Adv. Nano Res.*, **7**(3), 189-206. <http://dx.doi.org/10.12989/anr.2019.7.3.191>.
- Chaabane, L.A., Bourada, F., Sekkal, M., Zerouati, S., Zaoui, F.Z., Tounsi, A., Derras, A., Bousahla, A.A. and Tounsi, A. (2019), "Analytical study of bending and free vibration responses of functionally graded beams resting on elastic foundation", *Struct. Eng. Mech.*, **71**(2), 185-196. <https://doi.org/10.12989/sem.2019.71.2.185>.
- Chen, W. and Li, X. (2014), "A new modified couple stress theory for anisotropic elasticity and microscale laminated Kirchhoff plate model", *Arch. Appl. Mech.*, **84**(3), 323-341. <https://doi.org/10.1007/s00419-013-0802-1>.
- Chen, W., Li, L. and Xu, M. (2011), "A modified couple stress model for bending analysis of composite laminated beams with first order shear deformation", *Compos. Struct.*, **93**, 2723-2732. <https://doi.org/10.1016/j.compstruct.2011.05.032>.
- Cosserat, E. and Cosserat, F. (1909), *Theory of Deformable Bodies*, Hermann et Fils, Paris, France.
- El-Haina, F., Bakora, A., Bousahla, A.A., Tounsi A. and Mahmoud S.R. (2017), "A simple analytical approach for thermal buckling of thick functionally graded sandwich plates", *Struct. Eng. Mech.*, **63**(5), 585-595. <https://doi.org/10.12989/sem.2017.63.5.585>.
- Ezzat, M.A., El-Karamany, A.S. and El-Bary, A.A. (2017), "Two-temperature theory in Green-Naghdi thermoelasticity with fractional phase-lag heat transfer", *Microsyst. Technol.*, **24**(2), 951-961. <https://doi.org/10.1007/s00542-017-3425-6>.
- Ezzat, M.A., El-Karamany, A.S. and Ezzat, S.M. (2012), "Two-temperature theory in magneto-thermoelasticity with fractional order dual-phase-lag heat transfer", *Nucl. Eng. Des.*, **252**, 267-277. <https://doi.org/10.1016/j.nucengdes.2012.06.012>.
- Fahsi, A., Tounsi, A., Hebali, H., Chikh, A., Adda Bedia, E.A. and Mahmoud, S.R. (2017), "A four variable refined nth-order shear deformation theory for mechanical and thermal buckling analysis of functionally graded plates", *Geomech. Eng.*, **13**(3), 385-410. <https://doi.org/10.12989/gae.2017.13.3.385>.
- Fakhrabadi, S.M.M. (2017), "Application of modified couple stress theory and homotopy perturbation method in investigation of electromechanical behaviours of carbon nanotubes", *Adv. Appl. Math. Mech.*, **9**(1), 23-42. <https://doi.org/10.4208/aamm.2014.m71>.
- Fang, Y., Li, P. and Wang, Z. (2013), "Thermoelastic damping in the axisymmetric vibration of circular

- microplate resonators with two dimensional heat conduction”, *J. Therm. Stress.*, **36**, 830-850. <https://doi.org/10.1080/01495739.2013.788406>.
- Hadjefandiari, A.R. and Dargush, G.F. (2011), “Couple stress theory for solids”, *Int. J. Solid. Struct.*, **48**(18), 2496-2510. <https://doi.org/10.1016/j.ijsolstr.2011.05.002>.
- Karami, B., Janghorban, M. and Tounsi, A. (2019), “Galerkin’s approach for buckling analysis of functionally graded anisotropic nanoplates/different boundary conditions”, *Eng. Comput.*, **35**, 1297-1316. <https://doi.org/10.1007/s00366-018-0664-9>.
- Karami, B., Janghorban, M. and Tounsi, A. (2019a), “Wave propagation of functionally graded anisotropic nanoplates resting on Winkler-Pasternak foundation”, *Struct. Eng. Mech.*, **7**(1), 55-66. <https://doi.org/10.12989/sem.2019.70.1.055>.
- Kaur, H. and Lata, P. (2020a), “Effect of thermal conductivity on isotropic modified couple stress thermoelastic medium with two temperatures”, *Steel Compos. Struct.*, **34**(2), 309-319. <https://doi.org/10.12989/scs.2020.34.2.309>.
- Kaushal, S., Kumar, R. and Miglani, A. (2010), “Response of frequency domain in generalized thermoelasticity with two temperatures”, *J. Eng. Phys. Thermophys.*, **83**(5), 1080-1088. <https://doi.org/10.1007/s10891-010-0433-0>.
- Ke, L.L. and Wang, Y. S. (2011), “Size effect on dynamic stability of functionally graded micro beams based on a modified couple stress theory”, *Compos. Struct.*, **93**, 342-350. <https://doi.org/10.1016/j.compstruct.2010.09.008>.
- Koiter, W.T. (1964), “Couple-stresses in the theory of elasticity”, *Proc. Nat. Acad. Sci.*, **67**, 17-44.
- Kong, S., Zhou, S., Nie, Z. and Wang, K. (2008), “The size-dependent natural frequency of Bernoulli-Euler micro-beam”, *Int. J. Eng. Sci.*, **46**, 427-437. <https://doi.org/10.1016/j.ijengsci.2007.10.002>.
- Kumar, R. and Devi, S. (2016), “A problem of thick circular plate in modified couple stress theory of thermoelastic diffusion”, *Cogent Math.*, **3**(1), 1-14. <http://dx.doi.org/10.1080/23311835.2016.1217969>.
- Kumar, R., Sharma, N. and Lata, P. (2016b), “Effects of Hall current and two temperatures in transversely isotropic magneto-thermoelastic with and without energy dissipation due to ramp type heat”, *Mech. Adv. Mater. Struct.*, **24**(8), 625-635. <https://doi.org/10.1080/15376494.2016.1196769>.
- Kumar, R., Sharma, N. and Lata, P. (2016a), “Thermomechanical interactions due to Hall current in transversely isotropic thermoelastic medium with and without energy dissipation with two temperatures and rotation”, *J. Solid Mech.*, **8**(4), 840-858.
- Lata, P. (2018), “Effect of energy dissipation on plane waves in sandwiched layered thermoelastic medium”, *Steel Compos. Struct.*, **27**(4), 439-451. <http://doi.org/10.12989/scs.2018.27.4.439>.
- Lata, P. and Kaur, H. (2019a), “Deformation in transversely isotropic thermoelastic medium using new modified couple stress theory in frequency domain”, *Geomech. Eng.*, **19**(5), 369-381. <https://doi.org/10.12989/gae.2019.19.5.369>.
- Lata, P. and Kaur, H. (2019), “Axisymmetric deformation in transversely isotropic thermoelastic medium using new modified couple stress theory”, *Coupl. Syst. Mech.*, **8**(6), 501-522. <https://doi.org/10.12989/csm.2019.8.6.501>.
- Lata, P. and Kaur, H. (2020), “Effect of two temperature on isotropic modified couple stress thermoelastic medium with and without energy dissipation”, *Geomech. Eng.*, **21**(5), 461-469. <https://doi.org/10.12989/gae.2020.21.5.461>.
- Ma, H.M., Gao, X.L. and Reddy, J.N. (2008), “A microstructure-dependent Timoshenko beam model based on a modified couple stress theory”, *J. Mech. Phys. Solid.*, **56**, 3379-3391. <https://doi.org/10.1016/j.jmps.2008.09.007>.
- Ma, H.M., Gao, X.L. and Reddy, J.N. (2011), “A non-classical Mindlin plate model based on a modified couple stress theory”, *Acta Mechanica*, **220**(1-4), 217-235. <http://doi.org/10.1007/s00707-011-0480-4>.
- Marin, M. (1998), “Contributions on uniqueness in thermoelastodynamics on bodies with voids”, *Revista Ciencias Matematicas (Havana)*, **16**(2), 101-109.
- Marin, M. (2009), “On the minimum principle for dipolar materials with stretch”, *Nonlin. Anal.: Real World Appl.*, **10**, 1572-1578. <https://doi.org/10.1016/j.nonrwa.2008.02.001>.
- Marin, M., Ellahi, R. and Chirilă, A. (2017), “On solutions of Saint-Venant’s problem for elastic dipolar bodies

- with voids”, *Carpath. J. Math.*, **33**(2), 219-232.
- Medani, M., Benahmed, A., Zidour, M., Heireche, H., Tounsi, A., Bousahla, A.A., Tounsi, A. and Mahmoud, S.R. (2019), “Static and dynamic behavior of (FG-CNT) reinforced porous sandwich plate”, *Steel Compos. Struct.*, **32**(5), 595-610. <https://doi.org/10.12989/scs.2019.32.5.595>.
- Mehralian, F. and TadiBeni, Y. (2017), “Thermo-electromechanical buckling analysis of cylindrical nanoshell on the basis of modified couple stress theory”, *J. Mech. Sci. Technol.*, **31**(4), 1773-1787. <https://doi.org/10.1007/s12206-017-0325-8>.
- Othman, M.I.A. and Marin, M. (2017), “Effect of thermal loading due to laser pulse on thermoelastic porous medium under G-N theory”, *Result. Phys.*, **7**, 3863-3872. <https://doi.org/10.1016/j.rinp.2017.10.012>.
- Othman, M.I.A. and Abbas, I.A. (2012), “Generalized thermoelasticity of thermal-shock problem in a nonhomogeneous isotropic hollow cylinder with energy dissipation”, *Int. J. Thermophys.*, **33**(5), 913-923. <https://doi.org/10.1007/s10765-012-1202-4>.
- Othman, M.I.A., Atwa, S.Y., Jahangir, A. and Khan, A. (2013), “Generalized magneto-thermo-microstretch elastic solid under gravitational effect with energy dissipation”, *Multidisc. Model. Mater. Struct.*, **9**(2), 145-176. <https://doi.org/10.1108/MMMS-01-2013-0005>.
- Othman, M.I.A., Atwa, S.Y., Jahangir, A. and Khan, A. (2015), “The effect of gravity on plane waves in a rotating thermo-microstretch elastic solid for a mode-I crack with energy dissipation”, *Mech. Adv. Mater. Struct.*, **22**(11), 945-955. <https://doi.org/10.1080/15376494.2014.884657>.
- Park, S.K. and Gao, X.L. (2006), “Bernoulli-Euler beam model based on a modified couple stress theory”, *J. Micromech. Microeng.*, **16**, 2355. <https://doi.org/10.1088/0960-1317/16/11/015>.
- Park, S.K. and Gao, X.L. (2008), “Variational formulation of a modified couple stress theory and its application to a simple shear problem”, *Zeitschrift für Angewandte Mathematik und Physik*, **59**, 904-917.
- Press, W.H., Teukolsky, S.A., Vetterling, W.T. and Flannery, B.P. (1986), *Numerical Recipe*, Cambridge University Press.
- Rafiq, M., Singh, B., Arifa, S., Nazeer, M., Usman, M., Arif, S., Bibi, M. and Jahangir, A. (2019), “Harmonic waves solution in dual-phase-lag magneto-thermoelasticity”, *Open Phys.*, **17**(1), 8-15. <https://doi.org/10.1515/phys-2019-0002>.
- Sharma, N., Kumar, R. and Lata, P. (2015), “Disturbance due to inclined load in transversely isotropic thermoelastic medium with two temperatures and without energy dissipation”, *Mater. Phys. Mech.*, **22**(2), 107-117.
- Simsek, M., Kocaturk, T. and Akbas, S.D. (2013), “Static bending of a functionally graded microscale Timoshenko beam based on the modified couple stress theory”, *Compos. Struct.*, **95**, 740-747. <http://doi.org/10.1016/j.compstruct.2012.08.036>.
- Slaughter, W.S (2002), *The Linearised theory of Elasticity*, Birkhauser.
- Sobhy, M. and Radwan, A.F. (2017), “A new quasi 3D nonlocal plate theory for vibration and buckling of FGM nanoplates”, *Int. J. Appl. Mech.*, **9**(1), 1750008-29. <https://doi.org/10.1142/S1758825117500089>.
- Tsiatas, G.C. (2009), “A new Kirchhoff plate model based on a modified couple stress theory”, *Int. J. Solid. Struct.*, **46**, 2757-2764. <https://doi.org/10.1016/j.ijsolstr.2009.03.004>.
- Tsiatas, G.C. and Katsikadelis, J.T. (2009), “A BEM solution to the Saint-Venant torsion problem of micro-bar”, *Advances in Boundary Element Techniques X*, Eds. Sapountzakis, E.J. and Aliabadi, M.H., EC Ltd Publications, Eastleigh, UK, July.
- Yin, L, Qian, Q., Wang, L. and Xia, W. (2010), “Vibration analysis of microscale plates based on modified couple stress theory”, *Acta Mechanica Sinica*, **23**(5), 386-393. [http://dx.doi.org/10.1016/S0894-9166\(10\)60040-7](http://dx.doi.org/10.1016/S0894-9166(10)60040-7).
- Zarga, D., Tounsi, A., Bousahla, A.A., Bourada, F. and Mahmoud, S.R. (2019), “Thermomechanical bending study for functionally graded sandwich plates using a simple quasi-3D shear deformation theory”, *Steel Compos. Struct.*, **32**(3), 389-410. <https://doi.org/10.12989/scs.2019.32.3.389>.